Strange Particle Interactions In a Bubble Chamber

Peter Woit
Nicholas Carlin

Abstract:

We learned to identify many different kinds of particles in a hydrogen bubble chamber. Particular interest was focused on the strange baryons, Σ^+, Σ^-, and Λ°, produced in Kaon-nucleon interactions. A computer program was devised to locate points and determine particle tracks. This was used to measure the mass and lifetime of the Λ°, with results in agreement with the published values.

Excellent report WJF

THEORY OF STRANGE PARTICLE BUBBLE CHAMBER EXPERIMENTS

I Bubble Chambers[1]

Bubble chambers are one of the most effective ways of detecting elementary particles and measuring their properties. They are able to directly give the track followed by any charged particle that traverses them, and, when a magnetic field is used, the momentum of these particles can also be measured. In a typical experiment, a beam of high energy particles is sent into a bubble chamber, which is used simultaneously as a target for the beam and as a detector for the incident and scattered particles.

Bubble chambers contain a liquid at a temperature far above its boiling point, which is kept in the liquid state by an externally applied pressure. When this pressure is released, the liquid becomes superheated. The liquid then begins to boil preferentially along the ionization tracks of charged particles. At this point, photographs of the tracks of bubbles are taken from several angles by flash photography, thus allowing the reconstruction of the three dimensional paths of the particles in the bubble chamber.

Many different liquids have been used to make bubble chambers, but most chambers are of one of two types:

A. Cryogenic bubble chambers use the very lightest molecules: H_2, D_2, He, and operate at cryogenic temperatures. Most chambers of this type use liquid hydrogen. The main advantage of this is in the simplification of the interpretation of the experiment

since a high energy particle beam can only be significantly scattered by one type of particle: the proton. Thus, the H_2 bubble chamber provides a virtually pure proton target for the incident beam.

B. Heavy liquid bubble chambers use liquids such as propane, which do not require cryogenic operation. While these liquids provide a mixed target of protons and neutrons, they have one very significant advantage over H_2. While both types of bubble chamber are equally good at detecting charged particles, heavy liquids have the added advantage of being often able to detect neutral particles. This is possible since the neutral particle that is the most copiously produced in high energy collisions is the π^0 particle, which decays in around 10^{-16} seconds into two photons of high energy. As a result of the constraints of energy and momentum conservation, these high energy photons cannot form pairs of positive and negative charged particles unless they are able to exchange energy with the Coulomb field of a nucleus. If they are not able to do so, they will simply pass out of the bubble chamber undetected. For a liquid containing containing extremely light atoms such as H_2, this is what will generally happen. On the other hand, for a heavy liquid bubble chamber, especially if it is a large one, most of the high energy photons produced in particle reactions will be materialized into a positron-electron pair, which is readily recognizable as two tracks starting from the same point and spiralling in opposite directions in the magnetic field, losing energy by bremsstrahlung until they

both come to rest. In this way, the π^0's involved in particle reactions can generally be recognized, greatly aiding in the analysis of the reaction.

II Strange Particle Interactions

The table on the following page lists all the known particles of relatively low mass, along with their properties. The elementary particles are divided first of all into two categories: leptons, which can only interact through weak and electromagnetic forces, and hadrons, which are thought to consist of three types of quarks (up, down and strange), and are able to interact through the so-called "strong" force. The hadrons may be subdivided into those that contain a strange quark and those that don't; if a particle contains a strange quark, it is referred to as a strange particle.

Each of the three types of forces that can act between these particles has the property that certain numbers, integers called quantum numbers, can be assigned to the particles in such a way that these numbers will be additively conserved in any particle interaction. For example, the strangeness quantum number can be assigned in the following way: assign 1 to certain of the strange particles, -1 to their anti particles, and 0 to all non-strange particles. This strangeness number will be conserved by the electromagnetic and strong forces, but not by the weak forces. This conservation is due to the fact that weak forces are the only ones that can change strange quarks into up and down quarks, and vice-versa. The quantum number assignments are given in the table on the following page.[3]

		Charge	Mass (Mev)	lifetime (sec)	Baryon #	Strangeness
Leptons	electron	−1	.511		0	0
	positron	+1	.511		0	0
	μ^+	+1	105.66	2.212×10^{-6}	0	0
	μ^-	−1	105.66	2.212×10^{-6}	0	0
	$\nu, \bar{\nu}$	0	0		0	0
Hadrons	π^+	+1	139.6	2.55×10^{-8}	0	0
	π^-	−1	139.6	2.55×10^{-8}	0	0
	π^0	0	135.0	2×10^{-16}	0	0
	K^+	+1	493.9	1.22×10^{-8}	0	+1
	K^-	−1	493.9	1.22×10^{-8}	0	−1
	$k^0, \bar{K}^0$	0	497.8	2.6×10^{-8}	0	+1, −1
	p	+1	938.2		1	0
	$\bar{p}$	−1	938.2		−1	0
	n	0	939.5		1	0
	$\bar{n}$	0	939.5	1.1×10^{3}	−1	0
	$\Lambda^0, \bar{\Lambda}^0$	0	1115.6	2.5×10^{-10}	1, −1	−1, +1
	Σ^+	1	1189.4	$.81 \times 10^{-10}$	1	−1
	$\bar{\Sigma}^-$	−1	1189.4	$.81 \times 10^{-10}$	−1	+1
	$\Sigma^0, \bar{\Sigma}^0$	0	1191.5	$\ll 10^{-14}$	1, −1	−1, +1
	Σ^-	−1	1196.0	1.61×10^{-10}	1	−1
	$\bar{\Sigma}^+$	+1	1196.0	1.61×10^{-10}	−1	+1

1. The K^+ Particle

The K^+ is a particle with strangeness +1. Since there are no lighter particles with non-zero strangeness, it cannot decay by the strong or electromagnetic interactions, and must do so by the weak interactions, giving it the relatively long lifetime of 1.2×10^{-8} seconds. It can be produced in $\pi^+ P$ collisions, such as $\pi^+ p \rightarrow \Sigma^+ + K^+$. At energies below 500 Mev, K^+ P collisions can only produce elastic scattering, there are no other sets of particles with low enough threshold energy and the right quantum numbers to be produced by the strong force in a K^+ P collision. There are six principle decay modes, with the following branching ratios:

$K^+ \rightarrow \mu^+ \nu$	63.6 %
$K^+ \rightarrow \pi^+ \pi^0$	21.0 %
$K^+ \rightarrow \pi^+ \pi^- \pi^+$	5.6 %
$K^+ \rightarrow \pi^+ \pi^0 \pi^0$	1.7 %
$K^+ \rightarrow \mu^+ \pi^0 \nu$	3.2 %
$K^+ \rightarrow e^+ \pi^0 \nu$	4.8 %

2. The K^- Particle

The K^- is the antiparticle of the K^+, and it thus has opposite strangeness. Due to the particle-antiparticle symmetry of all known interactions, it has exactly the same decay modes and branching ratios as the K^+, except that all the decay products are replaced by their antiparticles. As a result of its strangeness of -1, K^- P collisions at 500 Mev can produce many different particles, unlike the K^+ case. The following will be the dominant ones:

$p + K^- \rightarrow \Lambda^0 + \pi^0$ ($\pi^0 \rightarrow 2\gamma$)

($\Lambda^0 \rightarrow p\pi^-$ or $n\pi^0$)

$p + K^- \rightarrow \Sigma^- + \pi^+$ ($\pi^+ \rightarrow \mu^+ \nu \rightarrow e^+ \nu\nu$)

($\Sigma^- \rightarrow n\pi^-$)

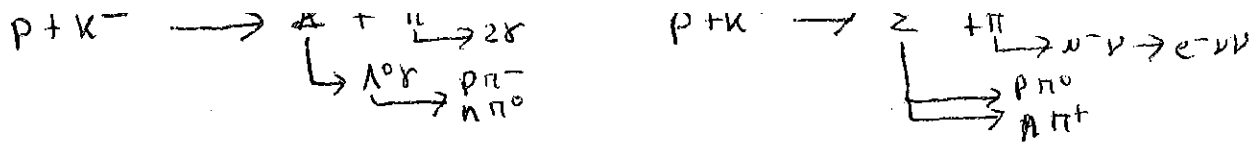

$$p + K^- \rightarrow p + K^-$$

THE EXPERIMENT

I K^+ Decays

Rolls of film taken from a propane bubble chamber at Argonne Laboratory were available. For each activation of the bubble chamber, views from three cameras, spaced at about 60 degrees from each other in an equilateral triangle, and looking into the bubble chamber through an optical window were projected and examined. A beam of K^+ particles entered the chamber, the magnetic field of which was such that they would come to rest near the center of the chamber. The K^+'s then decayed into one of six possible sets of particles, with the branching ratios given in the previous section.

The easiest decay mode to recognize was: $K^+ \rightarrow \pi^+ + \pi^+ + \pi^-$ This was the only decay mode that produced three charged particles, so the decay vertex looked like:

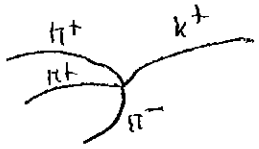

All the other decays had only one charged particle among the decay products, so the decay vertex looked like:

The $K^+ \rightarrow \mu^+ + \nu$ decay mode could be assumed to have occurred if no electron positron pairs were visible near the decay vertex,

however, this identification is not reliable since the photons from the π^0's might not have materialized.

The $K^+ \to \pi^+\pi^0\pi^0$ decay could only be reliably identified when three or four electron positron pairs were visible near the decay vertex.

The $K^+ \to \pi^+\pi^0$ decay could be reliably identified when a electron positron pair was seen that could be associated with the vertex, and when the charged secondary was seen to decay in two steps, first to a μ^+, then to a positron. Similarly, the $K^+ \to \mu^+\pi^0\nu$ and $K^+ \to e^+\pi^0\nu$ decays could be differentiated from the others by the fact that in the first case the charged secondary would decay once, in the second, it would not be seen to decay at all.

However, since information of the size of the bubble chamber and its magnetic field were not available, no accurate checks of momentum conservation at the decay vertices was possible, so no completely reliable particle identifications were possible for all the observed decays, so no reliable measurements of the branching ratios were possible. Thus our use of this film was limited to simply scanning for candidates for each of the decay modes, and we were able to find at least one event that fit the criteria above for each of the possible decays.

This sentence could use some work!

II K^- Reactions

The second part of our experiment involved the analysis of photographs taken at a hydrogen bubble chamber at Brookhaven laboratory. For this bubble chamber data on the positions of the fiducial markings on the glass window, as well as the

positions of the three cameras and the magnetic field, was available. This information is summarized in the next section. By calling Brookhaven, we determined that the optical window had a thickness of 3.914 inches, and was made of Corning BSC2 glass, with a refractive index of 1.517.

A beam of K^- particles, which from the measurements of some of their curvatures were determined to have energies of around 500 Mev, was incident on the bubble chamber from the right. The possible K^- P reactions at this energy were given in the previous section. The film was first scanned for Σ particle productions, which could be divided into three types:

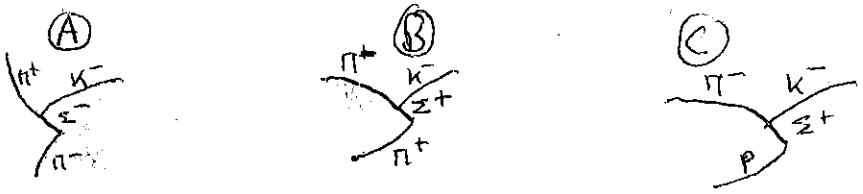

These different types of events were recognized by the curvatures of the tracks, which determined the charges of the particles involved. B and C were differentiated by the fact that the proton generally produced a shorter and thicker track than the π^+. In scanning 360 frames, 99 events of type A were observed, 32 events of type B, and 23 events of type C. Since the branching ratio of $K^+ \rightarrow \pi^+ n$ is about equal to that of $K^+ \rightarrow p\pi^0$ one would expect the number of B and C events to be equal, which was very roughly true, although the numbers involved are too small to say anything definite in this respect.

The film was next scanned for lambda productiona and decays. The Λ^0 decays 64.2% of the time into a p and a π^-, and 35.8% into a n and a π^0, which is not observable in a bubble chamber. The lambda can be produced in either of the following reactions:

$p + K^- \rightarrow \Sigma^0 + \pi^0$ ↳ $\Lambda^0 \gamma$ $\qquad$ $p + K^- \rightarrow \Lambda^0 + \pi^0$

These events had the following appearance in the bubble chamber.

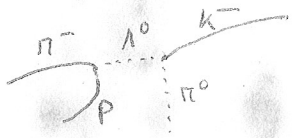

The bulk of the effort involved in our experiment went into the design on a method of accurately measuring these events and computing the mass and the lifetime of the lambda. The accuracy of these measurements was limited mainly by the inherent inaccuracies involved in measuring bubble chamber photographs on a projection screen. The following section describes the computer program.

Program Development

The information we needed to find the mass and lifetime of the Λ was: the position of the $K^- + p$ interaction, the position of the vertex, the curvature of the proton and pion tracks, and the angle between them.

Finding the spatial coordinates of a point using two cameras, and ignoring indices of refration, is fairly easy.

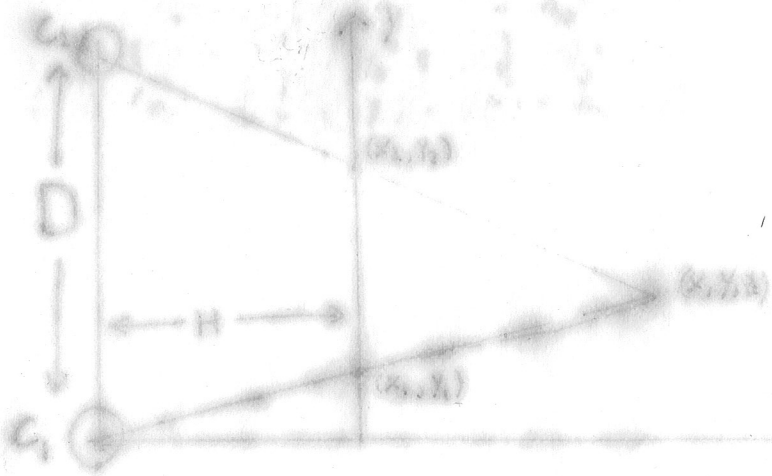

In fig.(1) D is the distance between the cameras, H the distance from the cameras' plane to the viewing plane. The coordinate origin is where the optic axis of C_1 meets the viewing plane, x_1, y_1, x_2, and y_2 are the coordinates of the point measured from each camera, and X, Y, and Z are the spatial coordinates of the point.

To find Y, simple trigonometry gives:

When these fomulae are calculated taking into account the glass window in the chamber and the index of refraction of the hydrogen and the glass, they become:

n_g and n_e are the index of refraction of the glass and the hydrogen respectively, and t is the thickness of the glass.

From the equations for X and Y, it seemed to us that any approximation that involved using the simpler equations with a modified H (as has been tried) would fail if t/ were non-negligable compared to 1. t (as we found out by calling Brookhaven- this should be in the lab manual) is 9.942 cm., is on the order of $n_g H$. n_g (also from Brookhaven) is 1.517, so $n_g H$ = 240 and t/ = .04 which is not negligable. We decided then, to use the exact formulae. Good

To get the index of refraction for the hydrogen we used the fact that n_e was 1.093 in a different bubble chamber with density = .059 gm./cc . is the electric susceptibility and is proportional to the number of dipoles/volume, and is then proportional to . According to the lab manual, =.062gm./cc. Scaling by .062/.059 gives n_e=1.0975.

We made our measurements with fiducial mark A at the origin and fiducial mark D on the positive x-axis (fig.(2)).

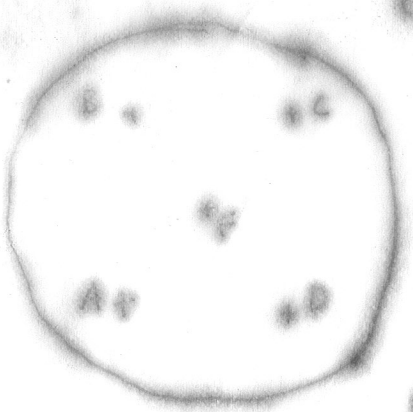

We had to then correct for the magnification of the film. this was accomplished by comparing the measured distance between the fiducials and the actual distance in the chamber. We used two slightly different magnification factors for the X and Y coordinates. Finally, the origin is translated to the optic axis of C_1.

This method gives the coordinates of a point in space, but it only uses two of the views. In order to make use of the other view the coordinate system is rotated and translated such that the other two camera-pair combinations in turn calculate the coordinates of the point in the same manner. (See the sample output. Settings 1, 2, and 3 refer to using camera pairs 1-3, 3-2, and 2-1 respectively.)

The error in determining the location of a point, as discussed in more detail later, comes mostly from measurement error. Slight changes in H, D, t, n_e, and n_g were found to have a much smaller effect than slight changes in the input coordinates. Comparing X, Y, and Z in the three settings is valuable then as an accuracy test: the more consistent the values, the more accurate they are. We found that the accuracy displayed on the sample printout was representative of the ones we used. (It should be noted that although in both the reaction and decay outputs the Z values of setting 1 are the highest, then 2, then 3, this pattern is not generally followed.)

The spread in Z is on the order of 1 cm., which makes an averaging procedure somewhat useless, so in the calculations to follow we used only setting one. This choice was made because the scanner for view 2 was slightly different than for views 1 and 3, and there are no rotations in and out of a different coordinate system to worry about.

Finding the angle and curvature required finding tangent vectors to the curves. This was done by drawing a tangent to the curve in one view, and using an iteration technique described by to find the corresponding point in the other view. The two lines of numbers in the printout under the third tangent point

input show the iterations of the corresponding point. As claimed by [illegible] they converge (to four decimal places) after just two iterations. Having these two vectors the angle between them is easily computed from [illegible].

The curvature of the traks was computed by a method adopted by us but developed (or at least used) by a previous group. This method corrects the observed curvature for the camera angle, and then chooses the median value for the radius to be used. This method is reasonable only for curves that are not too far out of the x-y plane. [illegible], the angle of the tangent vector out of the plane is useful for this purpose. ([illegible] $=\arctan(z/\sqrt{x^2+y^2})$ where x, y, and z are the components of the tangent vector.)

As a further diagnostic check, the percentage difference between the used view radius and the unused ones is calculated. In general we used only those events in which both [illegible] and these percentages were reasonably small.

Using this information, the momentum of the particles can be determined from: [illegible]

The cos [illegible] comes from the fact that the axis of the helix is in the z direction (because B is), therefore the measured [illegible] is only the projection of the actual [illegible] onto the x-y plane.

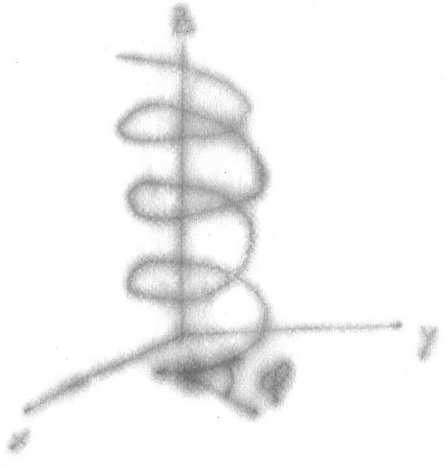

So, $\frac{v_\perp}{c} = \frac{qBr}{mc^2 \cos\phi}$

But $\gamma = \frac{1}{\sqrt{1-\frac{v^2}{c^2}}} \Rightarrow \frac{v^2}{c^2} = \frac{\left(\frac{qBr}{mc^2\cos\phi}\right)^2}{1+\left(\frac{qBr}{mc^2\cos\phi}\right)^2}$

and $p = \frac{mv}{\sqrt{1-\frac{v^2}{c^2}}}$. From this, $E = \sqrt{m^2c^4 + p^2c^2}$ is calculated.

So $m_{\Lambda^0} = \left[(E_p + E_\pi)^2 - (\vec{p}_p + \vec{p}_\pi)^2\right]^{1/2}$ with θ the angle between $\vec{p}_p$ and $\vec{p}_\pi$

If L is the calculated difference between the neutron point and the decay vertex, then

$$\tau = \frac{L m_{\Lambda^0} c}{p_{\Lambda^0} c}$$

Error Analysis

The two most important sources of error are in the measurement technique, and in the calculation of curvature.

To get a better idea of the practical difficulties in making these measurements, note first that, with the cameras placed where they are, measurements of the y-coordinate for a point should always be largest for view three and least for view one. Also, the x-coordinate for view two should be the smallest, and for views one and three about the same. We didn't realize this at first and, checking some later, we found several cases where these rules were violated, i.e. we had made a big mistake in measurement. These are extreme examples, but almost every time we went to recheck a measurement we had to change it slightly.

All in all, we figure our measurements to be good to about .1 cm., which translates to about .16cm. after magnification. If we believe the rotations in and out of the various settings to be exact, then the data shows a general uncertainty in the z-coordinate of about 1 cm. For lifetime measurements, however, where all we care about is the distance between points, since the two points are so close to each other, this uncertainty should be correlated in the two views, and therefore shouldn't cause a problem. Thus, the length measurement should be good to about .16cm.

The error in curvature is a bit harder to estimate. For radii of less than, say, 36 the template gives an accuracy of about 1. With the magnification that is about 1.6cm. Since the curvature subroutine only finds a best radius, and since the measured values are within 2 of each other, we can probably assume we're within 3 of the correct radius. This translates into around 15% error in p^2 or 7.5% in p.

In the mass formula then,

$$m_{ab}^2 = m_a^2 + m_b^2 - 2E_aE_b(\cos\theta + 2\sqrt{(m_a^2+p_a^2)(m_b^2+p_b^2)}$$

$$m_{ab}^2 \sim 10^2 \; ; \; m_p^2 \sim 10^4 ; \; 2E_aE_b\cos\theta \sim 10^2 ; \; 2\sqrt{\quad} \sim 10^5$$

So the major contribution to the error comes from the last term. A 15% error in p^2 gives a relative error of about 2% in m^2, or 1% in m. Therefore our values for the lambda mass should be within around 10 Mev.

In the lifetime formula,

$$\tau = \frac{\quad}{\quad}$$

the uncertainty in L is .16 cm. from before. In this event L was around 1 cm., implying a 16% error in L. Coupled with the 7.5% error in p and 1% error in m gives about 25% error in . So our calculated lifetimes should be good to $.65 \times 10^{-10}$ sec.

Data

Frame #	View #	Reaction Vertex (x, y)	Decay Vertex (x, y)	π^- Curvature	π^- distance	π^- tangent point (x, y)	p Curvature	p distance	p tangent point (x, y)
85	1	4.3, 18.35	3.4, 18.6	8.8	3	7, 23	34	7	-3, 19.9
	2	1.45, 20.3	.7, 20.55	6	4	1.6, 26	20	5.5	-5, 21
	3	4.5, 21.95	3.6, 21.85	8	5.5	6, 26.7	32	8	-4, 21.65
147	1	9.8, 12.5	9.5, 12.4	8	7	13.5, 10	40	5.5	2, 12.5
	2	7.45, 14.15	7.15, 14.1	7	7	12.1, 11	40	6	1, 13.9
	3	9.45, 15.55	9.7, 15.55	8.8	7	15, 13.2	38	5.5	5, 15.85
148	1	10.65, 1.5	10.65, 1.25	14	9	6, -2.4	26	5	-.1, 0
	2	6.6, 4.1	6.55, 3.85	14	10	.4, 0	24	5	0, 0
	3	10.7, 6.6	10.7, 6.3	12	8	5, 2.8	22	4	-3, 1
197	1	-6, 3.5	-5.6, 3	16	6	-8, 0	32	5	-7, 1
	2	-5.8, 4.65	-7.25, 4	16	6	-9.7, 1	40	6	-9.5, 3
	3	-5.9, 5.8	-5.5, 5	16	3	-7.1, 3	36	5	-7, 2
			-5.4, 6.8						
243	1	-7.2, 8.2	[illegible]	20	15	-4, 2	24	5	-5, 9.1
	2	-6.75, 8.95	-7.9, 8.4	24	15	-4.7, 0	19	5	-7, 10.3
	3	-7.9, 11.75	-8.3, 9.75	22	12	-3.65, 0	24	5	-5, 10.8

all dimensions in cm.

References

① C. Henderson, Cloud and Bubble Chambers, 1970

② David Rolson, ed Techniques of High Energy Physics, 1961

Pg.

③ Riccardo Levi-Setti, Elementary Particles, 1963

Results

Λ^0 particle

Frame #	θ_{proton}	θ_{pion}	$\cos\theta$	Mass of Λ (Mev)	Lifetime (10^{-10} sec)
85	-.67	.88	.65	1110.59	3.099
147	.16	.449	-.73	1099	1.378
148	.68	.41	.336	1107	1.044
197	-.3	-.08	-.133	1113.05	3.917
243	.09	-.4	.68	1122.7	4.56

Scatter here not consistent with 0.65 PVT

why does when error is 10

Average Mass: 1110.58 Mev ± 10 Mev

Average lifetime: 2.8×10^{-10} sec ± $.65 \times 10^{-10}$ sec

From table of particle properties: Mass of Λ: 1116.6 Mev

Lifetime of Λ: 2.6×10^{-10} sec

```
W

C:FCAL COMPILER V.BC1

  1.05 ZERO
  1.10 DIM C(3,2),AX(3),AY(3),NA(3),NB(3),NC(3),S(3),D(3)
  1.11 DIM A(3),B(3)
  1.12 DIM BX(3),BY(3),C0S(3),SIN(3),RV(3),DV(3,2),R(3),T(3),PIT(3)
  1.13 DIM SIN(3),COS(3)
  1.14 DIM PRT(3),DI(3),AC(5,3),DE(3)
  1.15 DIM P(3,2),PV(3,2)
  1.16 DIM XC(3),YC(3),VX(3),VY(3)
  1.18 DIM TP(3,2),TX(3)
  1.20 NG=1.517↑2;NE=1.0975↑2;H=157↑2;D(1)=60.2;D(2)=60.17;D(3)=60.17
  1.22 SIN(2)=FSIN(59.984*3.141593/180);COS(2)=-FCOS(59.984*3.141593/180
);SIN(3)=FSIN(60.032*3.141593/180)
  1.24 COS(3)=-FCOS(60.032*3.141593/180)
  1.26 T=9.942
  1.28 XC(1)=0;YC(1)=0;XC(2)=-52.1;YC(2)=30.1;XC(3)=0;YC(3)=60.2
  1.96 DIM M2(3)
  1.97 M2(1)=1.592;M2(2)=1.590;M2(3)=1.5936
  1.98 DIM M(3)
  1.99 M(1)=1.6;M(2)=1.587;M(3)=1.595

  2.05 A "HOW MANY EVENTS",NV
  2.10 IF E=NV; G 22
  2.12 Q=0;Q2=0
  2.15 E=E+1
  2.20 T "EVENT NUMBER",E,!
  2.25 G 10

  3.10 A "X(1)=",C(1,1);A "Y(1)=",C(1,2); A "X(2)=",C(2,1)
  3.15 A "Y(2)=",C(2,2);A "X(3)=",C(3,1);A "Y(3)=",C(3,2)
  3.20 D 4

  4.05 F V=1,3;I Q2<>2;D 35
  4.10 F I=1,3;I Q2=0;D 5
  4.15 IF Q2<>0;I=1;D 5;R

  5.01 C THIS SECTION COMPUTES THE POSITION OF A POINT IN THE BUBELE CHA
MBER
  5.10 I I=1;D 6.10
  5.11 I I=2;D 6.30
  5.12 I I=3;D 31
  5.15 ALF=FSQT((NG-1)*(AY(1)↑2+AX(1)↑2)+NG*H)
  5.20 BET=FSQT((NE-1)*(AY(1)↑2+AX(1)↑2)+NE*H)
  5.25 GAM=FSQT((NG-1)*((D(I)-AY(2))↑2+AX(2)↑2)+NG*H)
  5.30 DEL=FSQT((NE-1)*((D(I)-AY(2))↑2+AX(2)↑2)+NE*H)
  5.32 IF I=1; DO 9;I Q2=1; R
  5.35 NC(I)=BET*DEL*(ALF*GAM*(AY(2)-AY(1))+T*((AY(2)-D(I))*ALF-AY(1)*GA
M))/(ALF*GAM*(AY(1)*DEL-(AY(2)-D(I))*BET))
  5.40 A(I)=AX(1)*(1+T/ALF+NC(I)/BET)
  5.45 B(I)=AY(1)*(1+T/ALF+NC(I)/BET)
  5.50 I I=1;D 32
  5.51 I I=2;D 33
  5.52 I I=3;D 34
  5.60 T ! , "X,Y,AND Z IN SETTING",I,"ARE",NA(I),NB(I),NC(I)+T

  6.10 AX(1)=C(1,1);AY(1)=C(1,2);AX(2)=C(3,1);AY(2)=C(3,2);AX(3)=C(2,1);
AY(3)=C(2,2);R
  6.30 D 7;R
```

```
 7.20 J=1;K=2
 7.25 D 8
 7.30 J=2;K=1
 7.35 D 8
 7.40 J=3;K=3
 7.45 D 8

 8.10 AX(J)=COS(2)*C(K,1)-SIN(2)*C(K,2)
 8.20 AY(J)=SIN(2)*C(K,1)+COS(2)*C(K,2)+D(2)

 9.01 C THIS SECTION SAVES NUMBERS USEFUL IN THE TANGENT POINT COMPUTAT
ION
 9.05 PV(1,1)=AX(1);PV(1,2)=AY(1);PV(3,1)=AX(2);PV(3,2)=AY(2)
 9.10 A1=ALF;B1=BET;C1=GAM;D1=DEL

10.01 C DATA INPUT SECTION
10.02 Q=0
10.05 T !,"ENTER COORDINATES OF REACTION VERTEX",!
10.10 D 3
10.15 RV(1)=NA(1);RV(2)=NB(1);RV(3)=NC(1)
10.20 T !,"ENTER COORDINATES OF DECAY VERTEX",!
10.25 D 3
10.30 F I=1,3; F J=1,2; DV(I,J)=PV(I,J)
10.32 DE(1)=NA(1);DE(2)=NB(1);DE(3)=NC(1)
10.35 T !,"PION TRACK",!
10.40 G 10.55
10.45 Q=1
10.50 T !,"PROTON TRACK",!
10.55 D 11
10.60 D 12
10.65 I Q=0; D 15; G 10.45
10.70 PRR=R(N); F I=1,3;PRT(I)=T(I)
10.75 G 20

11.01 C THIS SECTION COMPUTES THE POSITION OF  A POINT ON THE TANGENT T
O THE TRACK
11.02 Y=10
11.04 Q2=1
11.05 FOR I=1,3; DO 14
11.06 D 4
11.07 F I=1,3;F J=1,2;TP(I,J)=PV(I,J)
11.10 V1=1;V2=3
11.12 DX1=TP(V1,1)-DV(V1,1);DY1=TP(V1,2)-DV(V1,2)
11.14 DX2=TP(V2,1)-DV(V2,1);DY2=TP(V2,2)-DV(V2,2)
11.15 X1=DV(V1,1)+Y*DX1/FSQT(DX1↑2+DY1↑2)
11.20 Y1=DV(V1,2)+Y*DY1/FSQT(DX1↑2+DY1↑2)
11.30 X2=DV(V2,1)+(X1-DV(V1,1))
11.35 Y2=DV(V2,2)+(DY2/DX2)*(X1-DV(V1,1))
11.37 Q1=0
11.40 Q1=Q1+1
11.42 T X2,Y2
11.56 AF=X1*(A1*C1*(B1-D1)+T*(B1*C1-A1*D1))
11.58 G=-(A1*C1*(Y1*(B1-D1)-60.2*B1)+T*Y1*(B1*C1-A1*D1))
11.60 K=-60.2*X1*(A1*B1*C1+T*(B1*C1-A1*D1))
11.62 S=(Y2-DV(3,2))/(X2-DV(3,1))
11.64 X2=-(AF*(DV(3,2)+S*(X2-DV(3,1)))+K)/G
11.66 Y2=DV(3,2)+S*(X2-DV(3,1))
11.68 IF Q1<6; G 11.40
11.72 C(1,1)=X1;C(1,2)=Y1;C(3,1)=X2;C(3,2)=Y2
11.80 Q2=2
11.82 D 4
11.84 TX(1)=NA(1);TX(2)=NB(1);TX(3)=NC(1)
11.90 T(1)=TX(1)-DE(1);T(2)=TX(2)-DE(2);T(3)=TX(3)-DE(3)
```

```
 12.01 C THIS SECTION COMPUTES THE RADIUS OF CURVATURE OF
 12.02 C THE TRACK
 12.05 PH=FSBR(30,T(3)/FSQT(T(1)↑2+T(2)↑2))
 12.10 F V=1,3; D 13
 12.15 I=FSGN(R(2)-R(3))*FSGN(R(1)-R(2))
 12.20 J=FSGN(R(2)-R(3))*FSGN(R(3)-R(1))
 12.25 N=2
 12.30 I J>=0; N=2-I; G 12.40
 12.35 I I<0; N=1
 12.40 T !,"PHI",PH
 12.45 T !,"XY RADIUS-",R(N),"    VIEW",N,!!
 12.50 F I=1,3; I I<>N; T "VIEW",I,"  ",(R(I)/R(N)-1)*100,"%  ",!

 13.01 C THIS SECTION CORRECTS THE OBSERVED CURVATURE FOR THE CAMERA ANG
LE
 13.05 VX=(XC(V)-DV(V,1))/184.25
 13.10 VY=(YC(V)-DV(V,2))/184.25
 13.15 TC=FSBR(30,(VX*T(2)-VY*T(1))/FSQT(T(1)↑2+T(2)↑2))
 13.20 TP=FSBR(30,(VX*T(1)+VY*T(2))/FSQT(T(1)↑2+T(2)↑2))
 13.25 T !,"ENTER RADIUS ON VIEW",V
 13.30 A A; A=A*20/(20/M(V))
 13.35 A "WHAT IS APPROX. DISTANCE OVER WHICH CURVE IS MEASURED",M
 13.40 DV=M*10/(20/M(V))
 13.45 A=FSBR(30,DV/A/FSQT(1-DV↑2/A↑2))/2
 13.50 SV=DV*FSIN(A)/FCOS(A)
 13.55 SA=SV/FCOS(TC)
 13.60 DA=FCOS(PH)*DV/FCOS(PH+TP)
 13.65 R(V)=DA/FSIN(2*FSBR(30,SA/DA))

 14.05 T !,"WHAT IS THE POSITION OF A POINT ON THE TANGENT LINE IN VIEW"
,I,!
 14.10 A,"X=",C(I,1)
 14.15 A,"Y=",C(I,2)

 15.05 PIR=R(N)
 15.10 F I=1,3; PIT(I)=T(I)

 20.01 C THIS SECTION COMPUTES COSINES AND LENGTHS
 20.05 NX=PRT(1); NY=PRT(2); NZ=PRT(3)
 20.10 CO=(NX*PIT(1)+NY*PIT(2)+NZ*PIT(3))/FSQT((NX↑2+NY↑2+NZ↑2)*(PIT(1)↑
2+PIT(2)↑2+PIT(3)↑2))
 20.11 T !"COS THETA",CO
 20.15 F I=1,3; DI(I)=RV(I)-DE(I)
 20.20 L=FSQT(DI(1)↑2+DI(2)↑2+DI(3)↑2)
```

```
 21.01 C THIS SEC COMPUTES AND TYPES OU THE INFORMATION FOR EACH EVENT
 21.05 PIA=3.8374*PIR/139.57/FCOS(PH)
 21.10 PRA=3.8374*PRR/938.26/FCOS(PH)
 21.15 PIV=FSQT(PIA↑2/(1+PIA↑2))
 21.20 PRV=FSQT(PRA↑2/(1+PRA↑2))
 21.25 PIP=FSQT(1/(1-PIV↑2))*139.57*PIV
 21.30 PRP=FSQT(1/(1-PRV↑2))*938.26*PRV
 21.35 PIE=FSQT(PIP↑2+139.57↑2)
 21.40 PRE=FSQT(PRP↑2+938.26↑2)
 21.45 T !,"EVENT NUMBER",E,!
 21.50 T !,"PION ENERGY",PIE,"MEV",!
 21.55 T !,"PROTON ENERGY",PRE,"MEV",!
 21.60 MA=FSQT((139.57)↑2+(938.26)↑2-2*PIP*PRP*CO+FSQT(4*((139.57)↑2+PIP
↑2)*((938.26)↑2+PRP↑2)))
 21.64 SPC=3E10
 21.65 LI=(FSQT(((139.57)↑2+(938.26)↑2+2*PIE*PRE+2*PIP*PRP*CO)/(PIP↑2+PR
P↑2+2*PIP*PRP*CO))*L/SPC)*1E10
 21.70 T !,"LAMBDA MASS",MA,"MEV",!
 21.75 T!,"LAMBDA LIFETIME",LI,"10↑-10 SECONDS",!
 21.80 MT=MT+MA; LT=LT+LI
 21.85 G 2.10

 22.01 C THIS AVERAGES THE VALUES FROM ALL THE EVENTS
 22.05 T !,"AVERAGE MASS",MT/NV,!
 22.10 T !,"AVERAGE LIFETIME", LT/NV,"10↑-10 SEC",!
 22.15 Q

 30.01 C THIS SUBROUTINE COMPUTES ARCTANGENTS
 30.05 Z1=1/FSQT(1+&↑2);Z2=1
 30.10 F Z3=1,10; Z1=(Z1+Z2)/2; Z2=FSQT(Z1*Z2)
 30.15 &=&/FSQT(1+&↑2)/Z1

 31.05 D 7
 31.10 BX(1)=COS(3)*AX(3)-SIN(3)*AY(3)
 31.15 BY(1)=SIN(3)*AX(3)+COS(3)*AY(3)+D(3)
 31.20 BX(2)=COS(3)*AX(1)-SIN(3)*AY(1)
 31.25 BY(2)=SIN(3)*AX(1)+COS(3)*AY(1)+D(3)
 31.30 F W=1,2; AX(W)=BX(W); AY(W)=BY(W)

 32.05 NA(1)=A(1);NB(1)=B(1)

 33.05 NA(2)=COS(2)*A(2)+SIN(2)*(B(2)-D(2))
 33.10 NB(2)=-SIN(2)*A(2)+COS(2)*(B(2)-D(2))

 34.05 MA=COS(3)*A(3)+SIN(3)*(B(3)-D(3))
 34.10 MB=-SIN(3)*A(3)+COS(3)*(B(3)-D(3))
 34.15 NA(3)=COS(2)*MA+SIN(2)*(MB-D(2))
 34.20 NB(3)=-SIN(2)*MA+COS(2)*(MB-D(2))

 35.05 P(V,1)=M(V)*C(V,1)
 35.10 P(V,2)=M2(V)*C(V,2)
 35.15 C(V,1)=P(V,1)-27.4
 35.20 C(V,2)=P(V,2)+10.1
#
```

```
#GO
HOW MANY EVENTS:1
EVENT NUMBER     1.0000

ENTER COORDINATES OF REACTION VERTEX
X(1)=:10.65
Y(1)=:1.5
X(2)=:6.6
Y(2)=:4.1
X(3)=:10.7
Y(3)=:6.6

X,Y,AND Z IN SETTING     1.0000ARE  -11.9870    14.4492    29.8498
X,Y,AND Z IN SETTING     2.0000ARE  -11.7339    14.6292    28.3862
X,Y,AND Z IN SETTING     3.0000ARE  -11.8509    14.8055    28.2905
ENTER COORDINATES OF DECAY VERTEX
X(1)=:10.65
Y(1)=:1.25
X(2)=:6.55
Y(2)=:3.85
X(3)=:10.7
Y(3)=:6.3

X,Y,AND Z IN SETTING     1.0000ARE  -11.9690    13.9677    29.5481
X,Y,AND Z IN SETTING     2.0000ARE  -11.7720    14.1521    28.6485
X,Y,AND Z IN SETTING     3.0000ARE  -11.8572    14.2328    28.4016
PION TRACK

WHAT IS THE POSITION OF A POINT ON THE TANGENT LINE IN VIEW     1.0000
X=:6
Y=:-2.4

WHAT IS THE POSITION OF A POINT ON THE TANGENT LINE IN VIEW     2.0000
X=:.4
Y=:0

WHAT IS THE POSITION OF A POINT ON THE TANGENT LINE IN VIEW     3.0000
X=:5
Y=:2.8
  -18.2146    15.3046  -18.2718    15.2695  -18.2718    15.2696  -18.2718
   15.2696  -18.2718    15.2696  -18.2718    15.2696
X,Y,AND Z IN SETTING     1.0000ARE  -21.6190     7.0337    34.7188
ENTER RADIUS ON VIEW     1.0000:14
WHAT IS APPROX. DISTANCE OVER WHICH CURVE IS MEASURED:9

ENTER RADIUS ON VIEW     2.0000:14
WHAT IS APPROX. DISTANCE OVER WHICH CURVE IS MEASURED:10

ENTER RADIUS ON VIEW     3.0000:12
WHAT IS APPROX. DISTANCE OVER WHICH CURVE IS MEASURED:8

PHI     0.4104
XY RADIUS-    22.1841     VIEW     1.0000

VIEW     2.0000      10.0401%
VIEW     3.0000     -23.5916%
```

```
PROTON TRACK

WHAT IS THE POSITION OF A POINT ON THE TANGENT LINE IN VIEW     1.0000
X=:12.5
Y=:-2

WHAT IS THE POSITION OF A POINT ON THE TANGENT LINE IN VIEW     2.0000
X=:8.35
Y=:0

WHAT IS THE POSITION OF A POINT ON THE TANGENT LINE IN VIEW     3.0000
X=:14
Y=:2
   -5.3678    13.6749    -5.4040    13.7221    -5.4040    13.7221    -5.4040
   13.7221    -5.4040    13.7221    -5.4040    13.7221
X,Y,AND Z IN SETTING     1.0000ARE   -6.5204     4.1219    38.7286
ENTER RADIUS ON VIEW     1.0000:26
WHAT IS APPROX. DISTANCE OVER WHICH CURVE IS MEASURED:5

ENTER RADIUS ON VIEW     2.0000:24
WHAT IS APPROX. DISTANCE OVER WHICH CURVE IS MEASURED:5

ENTER RADIUS ON VIEW     3.0000:22
WHAT IS APPROX. DISTANCE OVER WHICH CURVE IS MEASURED:4

PHI     0.6843
XY RADIUS-    27.7470     VIEW     3.0000

VIEW     1.0000      74.1492%
VIEW     2.0000      -3.1396%

COS THETA     0.3356
EVENT NUMBER     1.0000

PION ENERGY  177.6250MEV

PROTON ENERGY  948.2700MEV

LAMBDA MASS 1107.5000MEV

LAMBDA LIFETIME     1.044010↑-10 SECONDS

AVERAGE MASS 1107.5000

AVERAGE LIFETIME     1.044010↑-10 SEC
#
```